

Calculation of AC Loss for High Temperature Superconductor Transformers Using Two-Dimensional Finite Element Method

Asef Ghabeli Juybari^{1,1}, Mohammad Reza Besmi²

1 Faculty of Engineering, Shahed University, Tehran, Iran, Email:

Asefghabeli@yahoo.com

2 Faculty of Engineering, Shahed University, Tehran, Iran, Email:

Besmi@shahed.ac.ir

Abstract. The AC loss magnitude is one of the most important parameters for High Temperature Superconductor Transformer (HTS) design, which hysteresis loss forms its significant part. Leakage flux density includes two component: radial and axial, which its radial component plays an important role in hysteresis loss magnitude. In this paper, a shell-type HTS transformer with a very common P-S-P winding arrangement has been analyzed using finite element method. It should be mentioned that finite element analysis has been done using Cedrat Flux Ver 11.1 software. Then, hysteresis loss for this kind of winding arrangement has been calculated by means of simulation results.

Keywords: HTS Transformer, Hysteresis Loss, Leakage Flux, Finite Element Method.

1 Introduction

The introduction of high temperature superconductors has opened new horizons for practical use of superconducting in power devices such as transformers, cables, fault current limiters and etc [1]. In United States, transformers cause about 20 percent of total loss in transmission and distribution system [2]. Hence, using HTS transformers as an

¹ The Corresponding Author

alternative for conventional power transformers, can cause considerable energy saving and cost reduction [3, 4]. Furthermore, the weight and volume of HTS transformer is significantly reduced, compared with the conventional transformer. It is predicted that in United States, by 2020, about 80 percent of new power transformers, use superconductor instead of copper [5].

Many studies have been done to reduce AC losses in HTS transformers. Xiaosong Li et al. studied the effect of core geometry on leakage flux using finite element method [6, 7]. After simulation, it is concluded that there is almost no difference between the radial leakage flux of core type and shell type superconducting transformer.

The leakage flux around the transformer winding has two components. One of them is radial flux and the other is axial flux. The axial flux exists along the entire length of the winding. This kind of flux is parallel to the HTS tapes, so has no effect on the critical current of superconductor tape. The radial flux generates only at the winding ends and has significant effect on critical current of HTS tape because of its perpendicularity to it, and reduce the amount of critical current. In [8], the researchers diverted the magnetic field around the winding ends by using of Additional Ferromagnetic Rings (AFR) and could reduce the radial component of leakage magnetic field and consequently reduce the AC loss. Kim et al. could reduce the radial component of leakage flux in the HTS transformer, by designing a flux diverter that was placed between the primary and secondary winding [9]. Moreover in [10], the ac loss was reduced by designing an auxiliary winding which could reduce the radial leakage flux.

In the HTS transformers, the radial component of leakage flux has considerable effect in decreasing the critical current of superconductor winding, because it is perpendicular to HTS tape. So lots of researchers have tried to decrease this component by changing the arrangement of windings in HTS transformers. For instance, in [11], Xiaosong Li et al.

have studied the effects of unequal air gap between the coils of secondary pancake winding, on the radial and axial component of leakage flux. In [12], nine different commonly used winding arrangements in HTS transformers were compared to each other, and their ac loss were calculated by a finite element method based software; The calculation results showed that ac loss for cylindrical and helical windings are 3 to 12 times less than pancake windings. Also in [13], a new approach for ac loss reduction by means of a hybrid structure of S-P-S-P winding arrangement and auxiliary winding has been proposed. Researchers could decrease the radial component of leakage flux about 35%, by changing the location and sort order of each high and low voltage pancake in reciprocal winding arrangement; they also could decrease the radial leakage flux by increasing the number of pancakes which leads to decreasing the voltage per pancake [14].

In this paper, a 1 MVA 22.9/6.6 kV lowering transformer, with primary and secondary P-S-P concentric pancake winding arrangements has been simulated by Cedrat Flux software Ver. 11.1. The approach of simulating HTS transformer and superconductor tapes of its windings has been explained and discussed in details. From the results of this simulating, the axial and radial hysteresis loss and total hysteresis loss in the HTS windings was calculated.

2 Introduction to the superconductivity in HTS transformers

For defining the HTS material, firstly, the constitutive equation of the relation between B and H and also E and J should be determined. The magnetic flux density is defined as $B = \mu_0(H + M)$ where M is magnetization. In type II superconductors, the M definition is not straightforward. So the exclusion of magnetic flux in type II superconductors ($B=0$) can formulate in two different ways. To reach the relation $B=0$ inside the superconductor, either $H=-M$ and $H=M=0$

can be assumed. But it is more common to use the relation $H=M=0$, so the relation between B and H will be written as [15]:

$$B = \mu_0 H \quad (1)$$

The other constitutive equation is the relation between current density and electric field, which is often written as Ohm's law:

$$E = \rho(E, B) J \quad (2)$$

Where ρ is the resistivity.

The main problem to model a type II superconductor is the definition of its resistivity, because it is not constant and the Ohm's law will be nonlinear. For numerical modeling of HTS, the power-law model has usually been used. In addition to this fact that this model is more compatible with experimental results, it is a continuous function and easier to use for numerical formulation based on Maxwell's equations, because the numerical formulation for infinite conductivity of a material and also discontinuous functions is impossible [15].

For modeling the superconductor, the equation (3), which relates the electric field to the current density, has been used, that is called power-law model:

$$E = E_c \left(\frac{|J|}{J_{c(B)}} \right)^{n(B)-1} \frac{J}{J_{c(B)}} \quad (3)$$

From the Ohm's law and equation (3), the nonlinear resistivity of superconductor:

$$\rho(E, B) = \frac{E_c}{J_c(B)} \left| \frac{E}{E_c} \right|^{\frac{1-n(B)}{n(B)}} + \rho_0 \quad (4)$$

For describing the dependence of current density to perpendicular component of magnetic field density, the isotropic Kim-Anderson model has been used which is as follows [16]:

$$J_c(B, T) = \frac{J_{c0}(T)}{1 + \frac{|B|}{B_0}} \quad (5)$$

Where B is the magnitude of magnetic flux density, B_0 is a constant that is determined experimentally for each superconductor, $J_{c0}(T)$ is the critical current density in zero field that is depend on temperature.

3 AC Loss

Load losses of HTS transformers consist of hysteresis loss of superconductor tape, eddy current loss in silver matrix of superconductor tape, other stray loss due to eddy current loss in metallic parts of transformer like tank walls and other metal parts and finally the ohmic loss [17]. In HTS transformers the ohmic loss and the other mentioned losses are insignificant, and the major part of load loss is hysteresis loss of superconductor windings. This kind of hysteresis loss is due to anisotropic construction of superconductor tape, and the perpendicular component of leakage flux, which is perpendicular to the width of HTS tape, forms the significant part of it. The other component of leakage flux, which is parallel to the width of HTS tape, plays an insignificant role in the hysteresis loss value of superconductor tape [15, 18]. Hysteresis Loss per length unit, due to external magnetic field parallel to the width of HTS tape is as follows [19]:

$$\begin{cases} \frac{2fCA_c}{3\mu_0} B_p^3 & B_p < B_p \\ \frac{2fCA_c}{3\mu_0} B_p [3B_p - 2B_p] & B_p > B_p \end{cases} \quad (6)$$

Where C is coefficient of effective conduction area, A_c is the tape cross-sectional area, B_p is full penetration field flux density of superconductor tape, $B_{//}$ is the peak parallel flux density and f is the frequency.

Also, the hysteresis loss per length unit, due to external magnetic field perpendicular to the width of HTS tape is [19]:

$$P_{\perp} = Kf \frac{\pi\omega^2}{\mu_0} B_c B_{\perp} \left[\frac{2B_c}{B_c} \ln(\cosh \frac{B_{\perp}}{B_c}) - \tanh \frac{B_{\perp}}{B_c} \right] \quad (7)$$

Where ω is the width of HTS tape, B_c is the critical flux density, B_{\perp} is the peak perpendicular flux density and K is a geometrical parameter that represent the shape of HTS tape.

4 Overview of Finite Element Analysis

The finite element method (FEM) or finite element analysis (FEA) is a numerical analysis method for calculating partial differential equations. This analysis method is based on the complete elimination of steady state differential equations, or transferring the partial differential equations to the system. Nowadays, the application of this miniaturization method, in everyday life, such as engineering science, has become widespread, including the building design, calculating the cross-sectional area and perimeter of irregular objects. The finite

element method has a very high accuracy and has variety in analysis method such as manual calculation and computer simulating. The other benefits of this method are its compatibility with CAD/CAM applications. This method is able to physical modeling of the system with high accuracy, and by considering the structural and intrinsic details of it. In general, the steps of analyzing by finite element method are as follows [20-23]:

1. Modeling of the under study complicated object, by considering all of the physical, chemical, electrical, etc of constituent components of the object.
2. Splitting of the large object to the very little elements called “Mesh”, and studying the physical behavior of every mesh.
3. Integrating of meshes, by considering boundary conditions and constitution of the equation system for the whole complicated object.
4. Solving the equation system by considering the boundary conditions between elements.
5. Calculating the arbitrary parameters like force, inductance, and loss.

5 The Finite Element Modeling of the HTS Transformer

For optimization and loss reduction, the value and type of AC loss in different parts of transformer, should be exactly determined. But since the analytical methods of loss calculation, only exist for simple geometries, and on the other hand, these methods are not so accurate, so currently, numerical methods are pioneer for simulation and analyzing the AC loss in HTS field of research. One of the pioneer software is Cedrat Flux, which calculates electric, magnetic and thermal fields, based on finite element method. In this paper, Cedrat Flux has been used to simulate and analyze the AC loss in the HTS transformer.

5.1 Design of The HTS Transformer Geometry

The geometry design of this transformer is 2D, so the *xy* plate has been used for simulating. The modeling only includes the core and windings and do not includes the insulator parts of the transformer. For this purpose, a previously designed transformer by some of the researchers of Seoul National University in Korea, has been chosen [24]. The electrical characteristics and the dimensions of the simulated HTS transformer have been shown in table (1) and Figure (1), respectively. It should be mentioned that all the dimensions are based on millimeter scale.

Table 1. Electrical characteristics of simulated HTS transformer

Parameter	value	Unit
Power Rating	1	MVA
Rated Frequency	50	Hz
Rated Primary Voltage	22.9	kV
Rated Secondary Voltage	6.6	kV
Rated Primary Current	44	A
Rated Secondary Current	152	A
Number of Primary Turns	832	Turn
Number of Secondary Turns	240	Turn

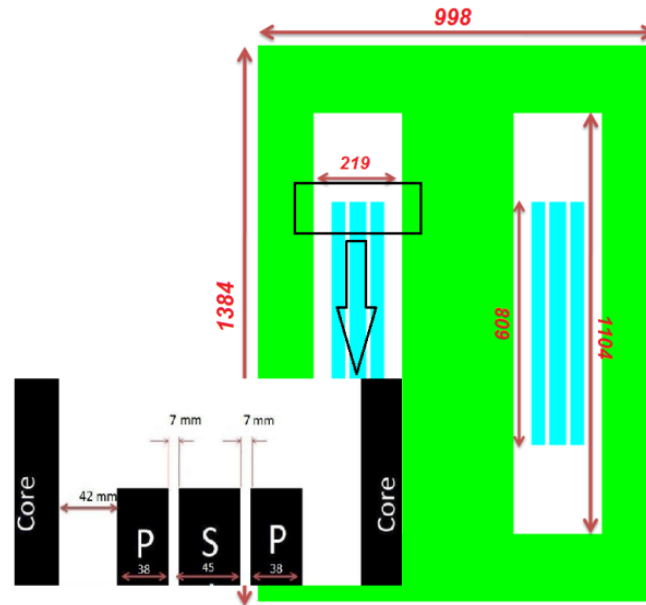


Fig. 1. Dimensions of the simulated HTS transformer

This transformer is a shell-type transformer and has concentric P-S-P windings and its coils have been wound as double pancake. In pancake type windings, that is a kind of disc type, the conductors are wound around as rectangular form. The double pancakes of secondary winding of this transformer, has been wound in 4 parallel paths, because the secondary rated current do not exceed the critical current of superconductor tape and quench does not occur. Firstly, the first primary coil with 416 turns, after that the secondary winding and finally the second primary coil with 416 turns, are wound concentrically one after each other, on the middle limb of transformer shell-type core. Because 2D modeling has been used in this paper, the under study primary and secondary windings are plotted as rectangular shapes, and each conductor is not shown separately.

5.2 Mesh Design and Boundary Condition

For mesh designing the plotted geometry in the software, three kinds of elements with different sizes have been selected. For the winding faces, small size elements, for the core face, medium size elements and for the face between the core and boundary lines, bigger size elements has been used. For the core face and regions around it, automatic meshing and for the winding faces, mapped meshing has been used. In winding meshing, because of using superconductor tapes and consequently much more leakage flux in winding surfaces, compared with the conventional copper windings, in addition to using smaller elements, the elements should be rectangular. It means that every element has 4 nodes, so the accuracy will be increased. The assigned mesh is shown in Fig. 2.

As it can be seen in Fig. 2, in the regions around the transformer core, the automatic meshing has been used. This kind of meshing is such that by getting away from the core, the element sizes become bigger and its number become fewer. This is because the fact that when the distance from the core is increased, the leakage flux density is getting lower and the flux lines become less dense, so to calculate the flux density distribution, less accuracy is needed. But in the regions close to the core or on the core and winding surfaces, the flux density is high, and to calculate the flux density distribution, more accuracy is needed. So the number of elements are high and their size is very small. Finally after complete meshing, 268357 nodes and 101362 elements have been created.

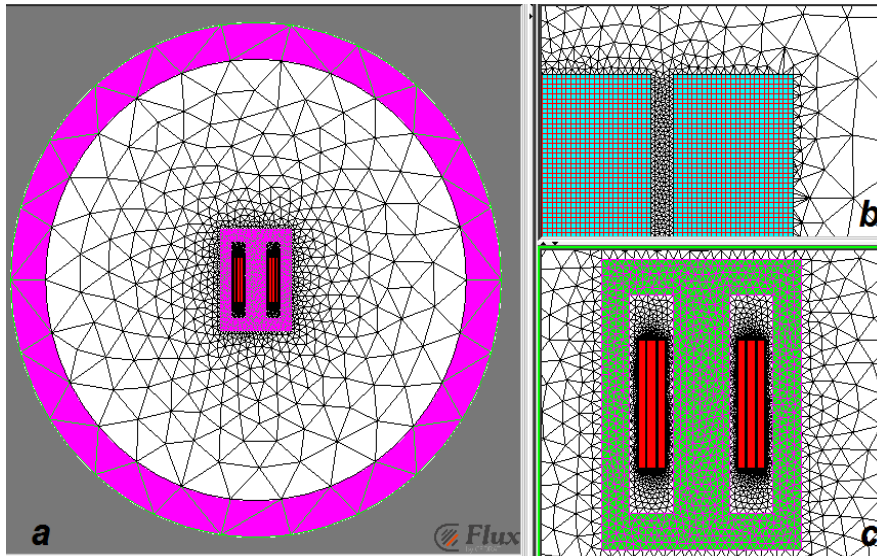


Fig. 2. An overview of assigned mesh in (a) Transformer, region around it and infinite box
(b) A part of winding (c) Transformer core

In this simulation, the dirichlet boundary condition has been used. In this kind of boundary condition, the magnetic vector potential on the boundary is zero ($\vec{A}=0$) and the magnetic field is tangent to the boundary.

5.3 Application Type

The purpose of this simulation is calculation of AC loss in the HTS transformer, and to calculate the AC loss the flux density distribution in the core and the regions around it and also in the superconductor winding, is needed. For this reason, the magneto-static application type can be used for analyzing the magnetic field and obtaining the flux density distribution.

5.4 Assigning the material

The next step in simulation of the HTS transformer by Flux 2D, is assigning the materials to each predefined region in the software. So, for the region around the core, the vacuum material is assigned, for the core region, silicon-steel sheets with the thickness of 0.291 mm, and B-H curve that has shown in table (2), is assigned.

The material of winding regions is superconductor. This material is introduced in the flux software by the constants such as E_c (critical electric field), J_c (critical current density at zero field), n_0 , ρ_0 (additional resistivity) and also B_0 and B_1 the constants for Kim-Anderson model. In table (3), the characteristics of BSCCO-2223 tape, used in the simulated transformer, has been shown.

Table 2. B-H characteristics of silicon-steel sheet

B	H	B	H
0	0	1.575	2754
0.7	98	1.591	3157
1.17	197	1.61	3549
1.26	295	1.63	3942
1.32	398	1.64	4321
1.38	590	1.66	4734
1.41	787	1.675	5126
1.465	1181	1.69	5534
1.5	1575	1.7	5907
1.525	1963	1.72	6307
	1.55		2362

Table 3. characteristics of BSCCO-2223 tape used in the simulated transformer

Quantity	Value	Unit
Thickness	0.31	mm
Width	4.1	mm
Critical Current (I_c)	135	A
Critical current density (B_c)	0.015	T
Full penetration field flux density (B_p)	0.0344	T
Effective conductor area (C)	0.77	-
Geometric parameter	1.35	-
Critical stress	265	MPa
Critical strain	0.4	%
Min. bend diameter	70	mm

Since in the simulated transformer, the superconductor tapes of windings, is floated in liquid nitrogen in 77 °C, the temperature variation assumed to be insignificant, and in the simulations J_c and n considered as temperature independent.

In the next step, to analyze the simulated transformer, an analysis scenario is created and the required setting is applied; such as the required precision for Newton-Raphson algorithm (the algorithm which is used for calculations) should be considered 1×10^{-6} . This means that the iteration method continues to the step that the difference between two successive iterations become less than 1×10^{-6} . The maximum number of iteration set to 500 iterations. This means that if the algorithm does not converge until 500th iteration, the calculations will be stopped. With these settings, solving the simulation with the magneto-static application will be started.

6 Simulation Results

After 1 minute processing with a system with Intel Core i5-2430M @ 2.4 GHz processor, and 4 GB RAM, the final solution has been obtained and the simulation solved completely.

In Fig. 4 flux density distribution and magnetic vector potential lines in the P-S-P winding is shown. As it can be seen, flux density magnitude in the core is 0.92. This magnitude does not relate to the winding type of transformer and is dependent on the magnitude of magnetizing current. In this simulation, the magnetizing current for this transformer is considered as zero, so the flux density in the core is very low and is different from operating point of the transformer. The flux density at the corners of the core is less than the other regions, because the flux density always tends to move in the paths with less magnetic reluctance.

In Fig. 5 flux density distribution in the windows and windings of the transformer with P-S-P winding has been shown. The maximum of leakage flux density, that is proportional to AC loss in the superconductor winding, is 53.33 mT. The value of leakage flux density in the region between the high and low voltage windings is maximum, because the leakage flux in this region is more than the other regions.

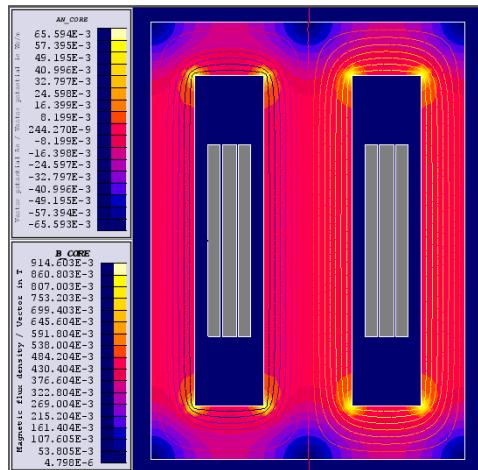


Fig. 4. Flux density distribution and magnetic vector potential lines in the core

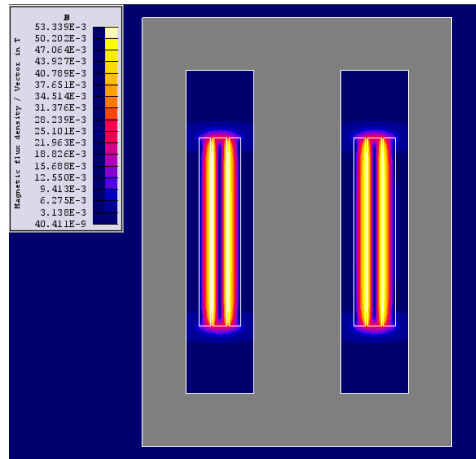


Fig. 5. Flux density distribution in the windows and windings of the transformer with P-S-P winding

In Fig. 6 radial flux density distribution in the windows and windings of the transformer with P-S-P winding has been shown. In the winding ends, the radial flux density is much more than the other regions, and by moving toward the winding center, the radial flux density become lower, until in the center of winding, that the flux density will be zero. This is because the fact that in the winding ends, the flux lines deviate from their vertical situation, so two components will be created: The radial component and the axial one. While in the other regions of winding (all regions except winding ends) only the axial component exist, because the flux lines are still vertical and has not deviated. For verification, as it can be seen in Fig. 7, in the central regions of windings, the axial component of flux has higher magnitude compared with the two ends of windings. On the other hand, the axial component of leakage flux in the regions between the low voltage winding and two coils of high voltage winding is higher than the other regions; because firstly the flux lines in these regions are more than the other regions, and secondly the primary and secondary currents are in

the opposite directions, so in the mentioned regions, the axial components of primary and secondary windings, reinforce each others.

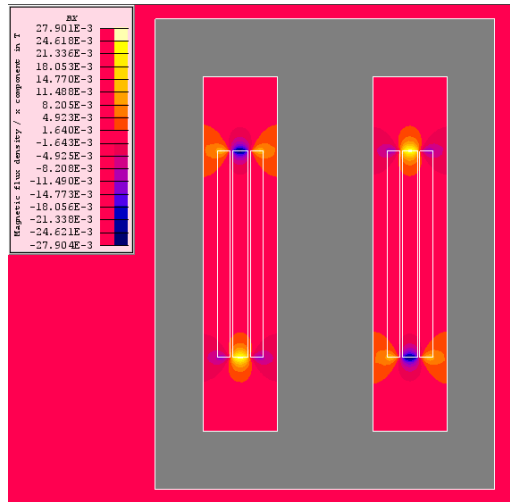


Fig. 6. Radial flux density distribution in the windows and windings of the transformer with P-S-P winding

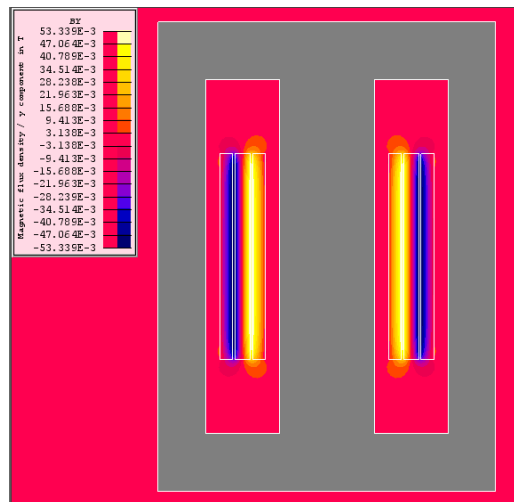


Fig. 7. Axial flux density distribution in the windows and windings of the transformer with P-S-P winding

The magnitude diagram of radial component of leakage flux in terms of distance along the height of the P-S-P winding has been shown in Fig. 8, and the magnitude diagram of axial component of leakage flux in terms of distance along the width of the P-S-P winding has been shown in Fig. 9.

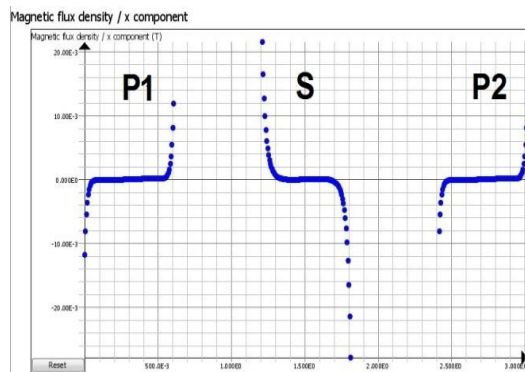


Fig. 8. Magnitude diagram of radial component of leakage flux in terms of distance along the height of the P-S-P winding

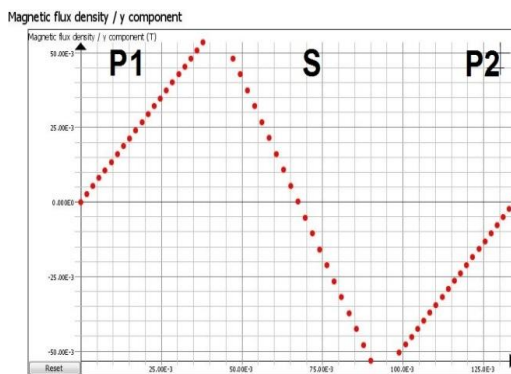


Fig. 9. Magnitude diagram of axial component of leakage flux in terms of distance along the width of the P-S-P winding

7 AC Loss Calculation

After the calculation of radial and axial leakage flux density distribution in the windings and obtaining the maximum value of radial and axial leakage flux density in each piece of primary and secondary windings, by using of equations (6) and (7) and also information of Table (3), the hysteresis loss in the HTS windings, will be calculated. After the calculation of hysteresis loss in terms of watt per meter in each piece, the length of each piece in terms of meter is multiplied by the hysteresis loss in each piece in terms of watt per meter. Then for the primary winding, the obtained hysteresis loss in two pieces of primary winding will be summed together so the total hysteresis loss in primary winding will be obtained. The results of calculations for the hysteresis loss has been shown in Table (4).

Table 4. Hysteresis loss in P-S-P winding in terms of watt

Type of hysteresis loss	Radial	Axial	Total
Magnitude of hysteresis loss	461.9	212.5	674.4

8 Conclusions

In this paper, a shell-type 1 MVA HTS transformer with pancake primary and secondary windings has been simulated by Cedrat Flux Ver. 11.1 software. Also, the approach of simulating HTS transformer and its superconductor tapes has been elaborated. Then, the figures of distribution of radial and axial leakage flux and magnetic vector potential lines has been shown and analyzed. It is concluded and verified that in the winding ends, the radial leakage flux density is much greater than the other regions, and the axial component of leakage flux density is higher at the center of the windings and also in

the air gaps between the secondary winding and two coils of primary winding. In the end, from the results of simulations, the radial, axial and total hysteresis loss in the HTS windings has been calculated.

References:

- [1] McConnell, B. W., "Transformers - a successful application of high temperature superconductors", IEEE Transactions on Applied Superconductivity, 2000, 10(1), 716-720. doi:10.1109/77.828332
- [2] Mehta, Sam P., Nicola Aversa, and Michael S. Walker. "Transforming transformers [superconducting windings]." *Spectrum, IEEE* 34, no. 7 (1997): 43-49.
- [3] McConnell, B. W., Mehta, S. P., & Walker, M. S., "HTS transformers", . IEEE Power Engineering Review, 2000, 20(6), 7-11. doi:10.1109/39.846102
- [4] Reis, C. T., Mehta, S. P., McConnell, B. W., & Jones, R. H., "Development of high temperature superconducting power transformers", Paper presented at the meeting of the IEEE Power Engineering Society Winter, 2002, January, Meeting, New York, N Y. doi: 10.1109/PESW.202.984977
- [5] Sheahen, T. P., McConnell, B. W., & Mulholland, J. W.. Method for estimating, "future markets for high-temperature superconducting power devices", IEEE Transactions on Applied Superconductivity, 2002, 12(2), 1784-1789. doi:10.1109/TASC.2002.1020337
- [6] Li, Xiaosong, Suping Wu, Yusheng Zhou, Gui Hu, and Guzong Long. "Influence of high temperature superconducting transformer geometry on leakage magnetic field." *Magnetics, IEEE Transactions on* 44, no. 4 (2008): 492-496.
- [7] Li, Xiaosong, Gui Hu, Guzong Long, Suping Wu, and Yusheng Zhou. "Analysis on magnetic field aimed at optimal design of HTS transformer." In *Automation Congress, 2008. WAC 2008. World*, pp. 1-4. IEEE, 2008.
- [8] Zizek, F., Z. Jelinek, Z. Timoransky, H. Piel, F. Chovanec, P. Mozola, and M. Polak. "End-winding region configuration of an HTS transformer." *Applied Superconductivity, IEEE Transactions on* 12, no. 1 (2002): 904-906.

- [9] Kim, S. H., W. S. Kim, W. G. Min, C. B. Park, S. J. Lee, J. T. Kim, D. K. Lee et al. "Analysis of perpendicular magnetic fields on a 1 MVA HTS transformer windings with flux diverters." *Applied Superconductivity, IEEE Transactions on* 14, no. 2 (2004): 932-935.
- [10] Heydari, Hossein, Faramarz Faghihi, and Reza Aligholizadeh. "A new approach for AC loss reduction in HTS transformer using auxiliary windings, case study: 25 kA HTS current injection transformer." *Superconductor Science and Technology* 21, no. 1 (2008): 015009.
- [11] Li, Xiaosong, Qiaofu Chen, Jianbo Sun, Yu Zhang, and Guzong Long. "Analysis of magnetic field and circulating current for HTS transformer windings." *Applied Superconductivity, IEEE Transactions on* 15, no. 3 (2005): 3808-3813.
- [12] Daneshmand, Shabnam Vahdati, Hossein Heydari, and Sadegh Shakeri, "Multicriteria Optimal Winding Scheme in HTS Transformers by Analytical Hierarchy Process." *Applied Superconductivity, IEEE Transactions on* 21, no. 1 (2011): 2-12.
- [13] Daneshmand, Shabnam Vahdati, and Hossein Heydari. "Hysteresis Loss Improvement in HTS Transformers Using Hybrid Winding Schemes." *Applied Superconductivity, IEEE Transactions on* 22, no. 2 (2012): 5500307-5500307.
- [14] Park, Chan-Bae, Woo-Seok Kim, Kyeong-Dal Choi, Hyeong-Gil Joo, Gye-Won Hong, and Song-Yop Hahn. "Optimization of 1 MVA high T_c superconducting transformer windings." *Applied Superconductivity, IEEE Transactions on* 13, no. 2 (2003): 2294-2297.
- [15] Stavrev, Svetlomis. "Modelling of high temperature superconductors for AC power applications." PhD diss., ÉCOLE POLYTECHNIQUE FÉDÉRALE DE LAUSANNE, 2002.
- [16] Y. B. Kim, C. F. Hempstead and A. R. Strnad, "Critical persistent currents in hard superconductors", *Phys. Rev. Lett.* 9 (7), p. 306, 1962
- [17] Carr, Walter James, "AC loss and macroscopic theory of superconductors", CRC Press, 2001.
- [18] Rabbers, J.J., AC Loss in Superconducting Tapes and Coils. 2001, University of Twente.

- [19] Wolfbrandt, Anna, Niklas Magnusson, and Sven Hornfeldt. "Losses in a BSCCO/Ag tape carrying AC transport currents in AC magnetic fields applied in different orientations." *Applied Superconductivity, IEEE Transactions on* 11, no. 4 (2001): 4123-4127.
- [20] M. N. O. Sadiku, "A Simple Introduction to Finite Element Analysis of Electromagnetic Problems", IEEE Transactions on Education, Vol. 32, No. 2, May 1989, pp. 85-93.
- [21] M. N. O. Sadiku, "Numerical Techniques in Electromagnetics", 2nd Edition, CRC Press LLC, 2001.
- [22] P. G. Ciarlet, "The Finite Element Method for Elliptic Problems", Amsterdam: North-Holland, 1978.
- [23] Mohammad Yazdani-Asrami, M. Mirzaie, A. Shayegani Akmal., No-Load Loss Calculation of Distribution Transformers Supplied by Nonsinusoidal Voltage Using Three-Dimensional Finite Element Analysis, *Energy* , Vol. 50, No. 1, February 2013, pp. 205-219.
- [24] Kim, Woo-Seok, Song-Yop Hahn, Kyeong-Dal Choi, Hyeong-Gil Joo, and Kye-Won Hong. "Design of a 1 MVA high T_c superconducting transformer." *Applied Superconductivity, IEEE Transactions on* 13, no. 2 (2003): 2291-2293.